



XPS and transmission electron microscopy of the multicomponent hydride-forming alloys for electrochemical applications

V.D. Dobrovolsky, Yu.M. Solonin*, V.V. Skorokhod, O.Yu. Khizhun

The Institute for the Problems of Material Science, NAS of Ukraine, Krzhizhanovsky, 3, 252680, Kiev, Ukraine

Abstract

Photoelectron spectra of the Ce4d, Ni2p, Ni3p, Co3p, Al2p, O1s, C1s in $Mm(Ni,Co,Al)_5$ and Zr3d, Ti2p, V2p, Ni2p, O1s, C1s in $Zr_{1-x}Ti_x(Ni,V,Co,Cr)_2$ alloys have been obtained. In the surface layer, about 2–2.5 nm of both alloys, the main part of the nickel atoms are in the metallic state (Ni^0) and only a third of them in oxidized states (Ni^{+2} , Ni^{+3}). At the same time the concentration of nickel in surface layer of Zr-content alloy is much smaller when compared with Mm-content alloy. The chemical state of the Co and V atoms is similar to the Ni atoms state, but their concentrations, especially of V, in the surface layer is smaller than that of nickel. The results of XPS have been compared with the data of transmission electron microscopy of the thin foils of La- and Zr- based alloys. Dark field microphotographs of the oxidized alloys indicate the presence of two different phases, which, according to electron microdiffraction, are nickel-based alloy and oxide. In the first stage of oxidation on the surface of the foil, fine nickel particles (about 10 nm) and an amorphous oxide phase appear. Complete oxidation of the foil leads to the formation of a eutectic like structure consisting of a mixture of metallic and oxide phases. Some difference in the oxidized layer structure of the investigated alloys has been observed.

Keywords: Hydrogen; Intermetallics; Batteries

1. Introduction

The alloys of the $La(Mm)Ni_{5-x}Me_x$ and $Zr_{1-x}Ti_x(Ni,V,Me)_2$ types are perspective electrode materials for rechargeable batteries. Each component of these alloys accounts for a certain bulk or surface property. If the bulk properties are determined by an average alloy composition, the surface properties depend on a redistribution of the elements in the surface layer and their interaction with a surrounding sphere. So, the alloys with similar bulk characteristics, such as equilibrium hydrogen pressure and hydrogen capacity, may exhibit different real electrochemical activity because of different surface states. The main process which influences alloy activity is the formation of a thin surface oxide layer and related element redistribution during exposure of the alloys to air [1,2].

The aim of this investigation is to determine the composition and structure of the surface oxide layer of the above mentioned multicomponent alloys, which demon-

strate different behavior during electrochemical hydriding-dehydriding. If the $La(Mm)Ni_{5-x}Me_x$ alloys have reached the nominal electrochemical capacity already after 1–3 cycles, the Zr-based alloys require special treatment for activation and 10–20 cycles [3,4].

2. Experimental details

The alloys $MmNi_{3.5}Co_{0.7}Al_{0.8}$ and $Zr_{0.59}Ti_{0.41}V_{0.53}Cr_{0.22}Fe_{0.20}Co_{0.27}Ni_{0.78}$ have been prepared by arc melting. The powders of these alloys were pressed to obtain pellets with $d=10$ mm, $h=2$ mm. Before investigation the samples were cleaned by Ar^+ sputtering for 5 min. The XPS analysis was performed on a ES-240 spectrometer at 2.10^{-7} Pa using $MgK\alpha$ radiation (Au 4f at 84.0 eV; 1.1 eV full width half maximum). XPS spectra of Ar^+ cleaned samples and samples exposed to air was obtained. For transmission electron microscopy (TEM) the $LaNi_{4.5}Al_{0.5}$ ($La(Mm)Ni_{5-x}Me_x$ type alloy) and above mentioned Zr-based alloy (Sapru alloy type) were used. Thin foils were prepared by ion beam thinning. The dark

*Corresponding author.

field images and selected area electron diffraction (SAED) of the air exposed samples were studied.

3. Results

The core levels Ni2p, Ni3p, Co2p, Al2p, O1s, C1s of $\text{MmNi}_{3.5}\text{Co}_{0.7}\text{Al}_{0.8}$ (Fig. 1) and Zr3d, Ti2p, Ni2p, V2p, O1s, C1s of $\text{Zr}_{0.59}\text{Ti}_{0.41}\text{V}_{0.53}\text{Cr}_{0.22}\text{Fe}_{0.20}\text{Co}_{0.27}\text{Ni}_{0.78}$ (Fig. 2) were analyzed. In a surface layer of about 2–3 nm for both alloys exposed to air the main part of nickel atoms are in metallic state Ni^0 (peak at 852.85 eV) and only a third of them are in oxidized state: Ni^{2+} and Ni^{3+} (peak at 855.75 eV). At the same time a comparison of the Ni-peak intensity/background intensity ratios indicates, that the concentration of nickel in the surface layer of the Zr-based alloy is much smaller when compared with the Mm-content alloy.

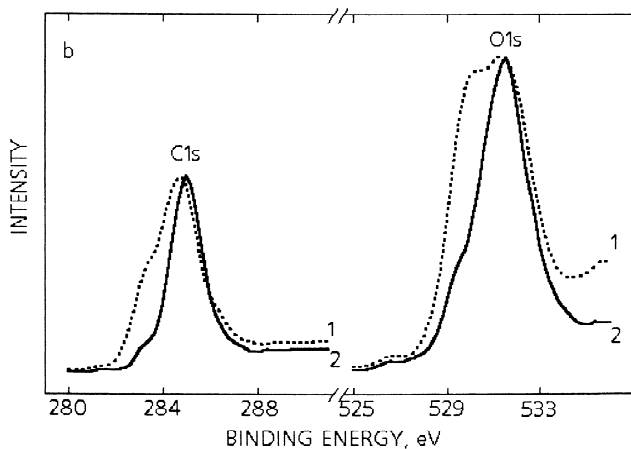
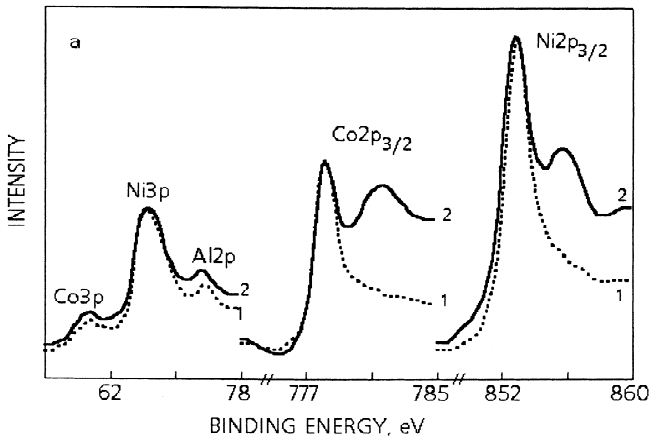


Fig. 1. The XPS spectra of Ni2p, Ni3p, Co2p, Al2p, Co3p (a) and O1s, C1s (b) of $\text{MmNi}_{3.5}\text{Co}_{0.7}\text{Al}_{0.8}$ alloy after Ar^+ sputtering (1) and exposure to air (2).

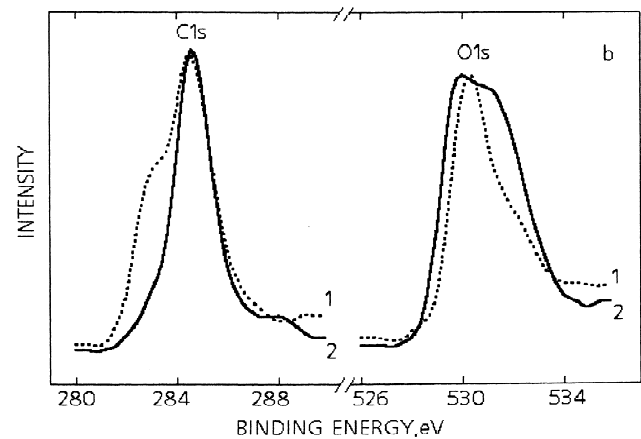
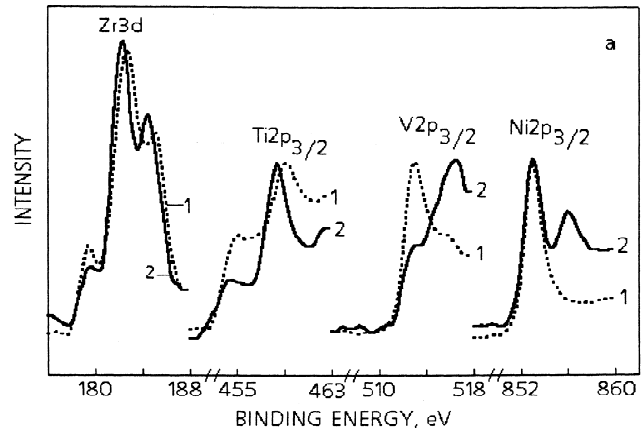


Fig. 2. The XPS spectra of Zr3d, Ti2p, Ni2p, V2p (a) and O1s, C1s (b) of $\text{Zr}_{0.59}\text{Ti}_{0.41}\text{V}_{0.53}\text{Cr}_{0.22}\text{Fe}_{0.20}\text{Co}_{0.27}\text{Ni}_{0.78}$ alloy after Ar^+ sputtering (1) and exposure to air (2).

The chemical states of Co and V and their change during exposure to air is similar to Ni, but the concentration of these metals, especially of V, is smaller than that of Ni (Figs. 1 and 2(a)). The part of the atoms in Me^0 state in surface layer of air exposed alloys decreases in the row Ni, Co, V. On the surface of $\text{MmNi}_{3.5}\text{Co}_{0.7}\text{Al}_{0.8}$ Al exists only in oxidized state (Fig. 1(a)).

$\text{Zr}_{0.59}\text{Ti}_{0.41}\text{V}_{0.53}\text{Cr}_{0.22}\text{Fe}_{0.20}\text{Co}_{0.27}\text{Ni}_{0.78}$ alloys both cleaned and exposed to air show mainly an oxidized state of Zr and Ti (Fig. 2). The presence of some metallic Zr (peak at 179 eV) and Ti (peak at 454 eV) indicates that the oxide layer is thinner than the XPS probing depth (2–3 nm).

The behavior of two O1s peaks of Mm-content alloy (Fig. 1(b)) is similar to that described in [5]. The peak at 530 eV may be attributed mainly to La_2O_3 . The peak at 531.5 eV may be attributed to metal hydroxides or other oxygen-content surface groups, which also may be respon-

sible for inhibition of surface electrochemical processes. The formation of such groups is not so clearly observed in Zr-based alloy (Fig. 2(b)).

Some effect was observed in the C1s spectra. Besides a peak at 283.6 eV the strong peak at 285.1 eV appears especially in alloys exposed to air. This peak may be attributed to hydrocarbons [5].

The transmission electron microscopy of $\text{LaNi}_{4.5}\text{Al}_{0.5}$ reveals three stages of alloy degradation during exposure to air. On the first stage on SAED besides diffraction spots from initial alloy one can observe the diffuse diffraction rings from the fine nickel particles (Fig. 3(a)). During further exposure to air the alloy oxidation develops and on a dark field image, obtained in Ni reflex the Ni particles of about 100 Å can be clearly observed (Fig. 3(b), (c)). The third stage diffraction spots from the initial alloy disappear and SAED consists of diffraction rings attributed to a mixture of La_2O_3 and Ni (Fig. 4(b)). The dark field images obtained in La_2O_3 and Ni reflexes separately show the eutectic-like two phase structure of the oxidized alloy foil (Fig. 4(a), (c)).

The two types of SAED from air exposed Zr-based alloy in the form of diffraction rings were observed. The first one was obtained from thin films attached to the edge of bulk alloy and attributed to TiO_x with cubic structure and $a=0.420$ nm. A similar diffraction pattern was described in [4]. The second one was obtained from the edge of the bulk alloy in the form of very diffuse rings attributed to a rutile-like structure.

4. Discussion and conclusion

Comparison of the XPS and TEM data shows that at the earliest stage of surface oxidation for the $\text{La}(\text{Mm})\text{Ni}_{5-x}\text{Me}_x$ type alloys very fine Ni particles form. These particles serve as a catalyst for hydrogen recombination and charge acceptance, providing high electrochemical activity. At the same time on the surface of Zr-based alloy, free Ni is covered by a compact layer of Zr and Ti oxides

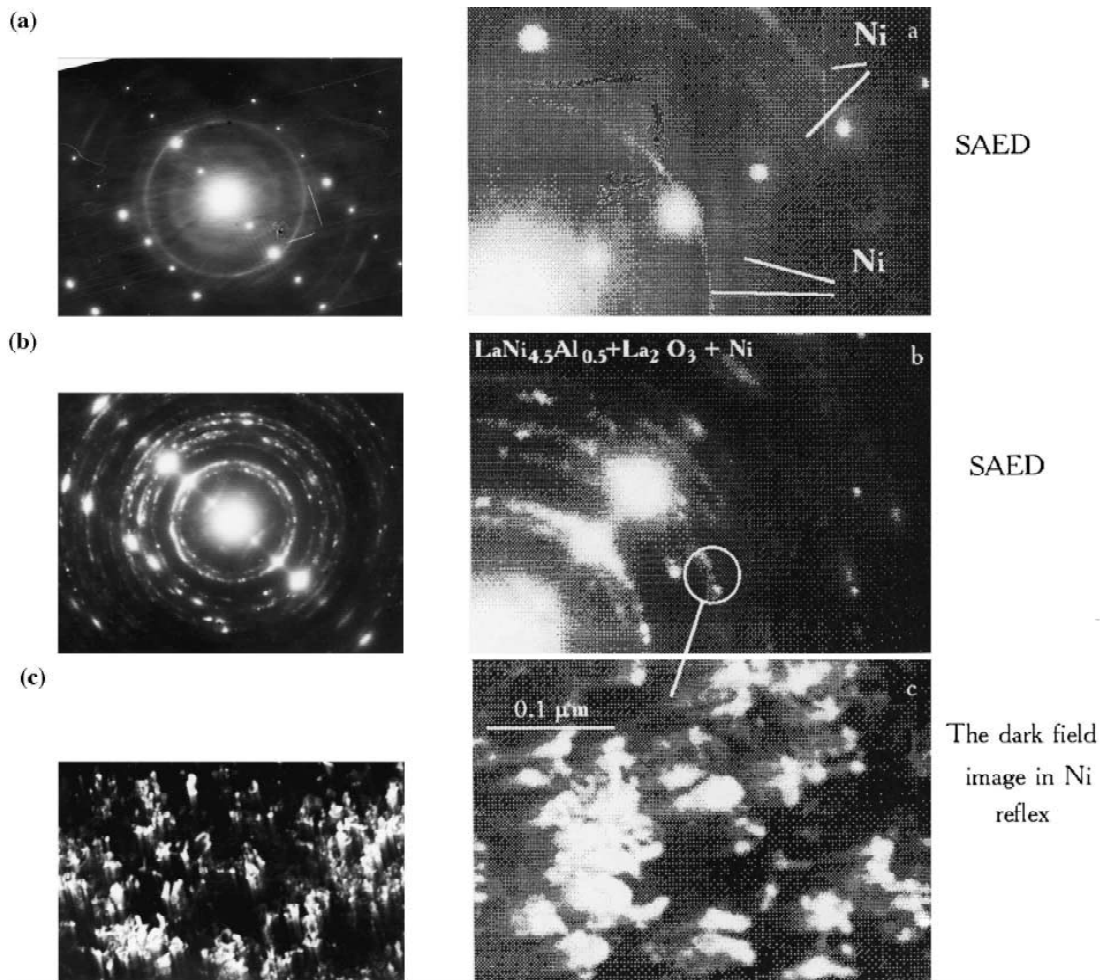


Fig. 3. The SAED (a, b) and dark field image in Ni (c) reflex of the oxidized $\text{LaNi}_{4.5}\text{Al}_{0.5}$ foil. First stage.

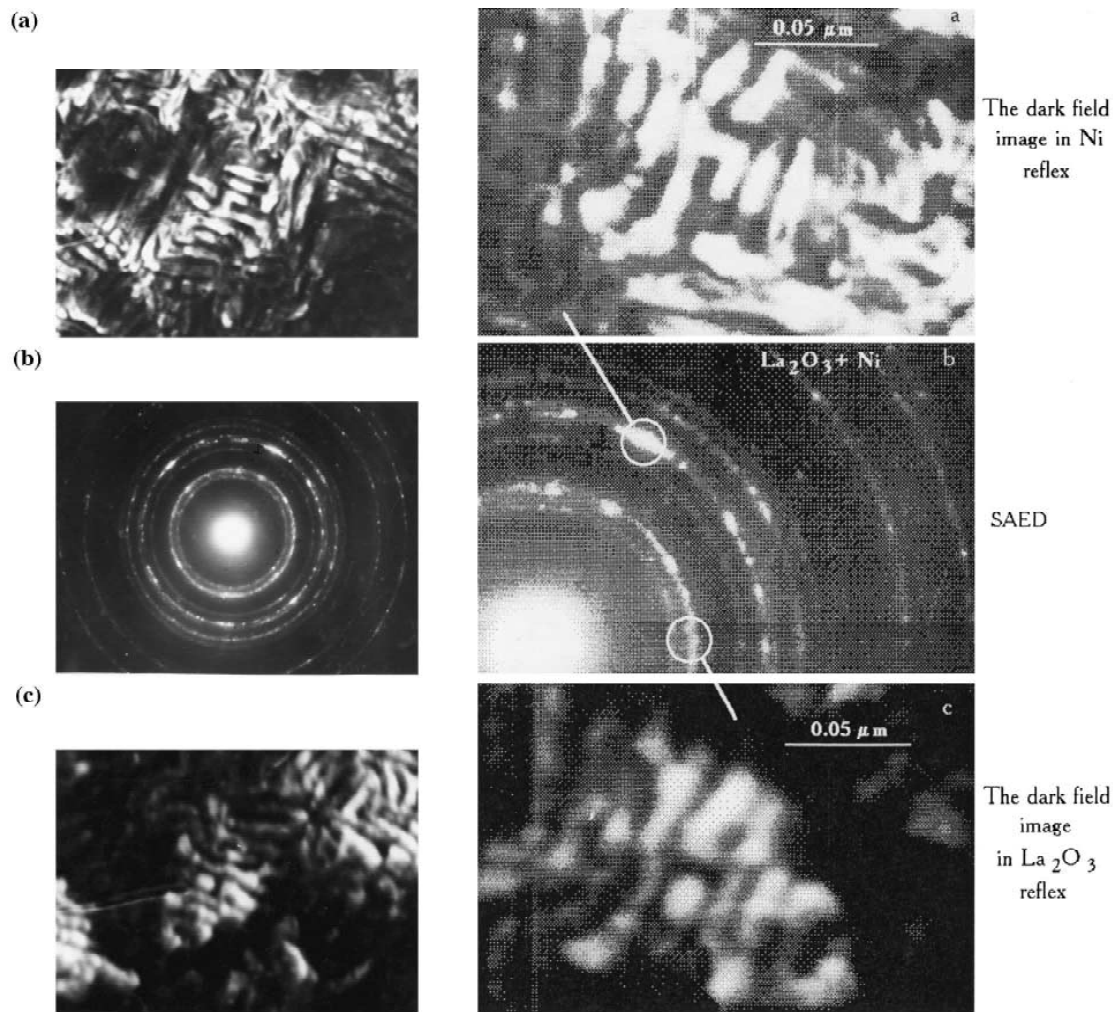


Fig. 4. The SAED (b) and dark field images in Ni (a) and La₂O₃ (c) reflexes of the oxidized LaNi_{4.5}Al_{0.5} foil. Second stage.

and only its destruction may lead to alloy activation. It must be emphasized that the role of surface oxygen- and carbon-content groups in the inhibition of the hydrogen chemisorption needs further investigation, maybe with the use of mass spectrometry.

Acknowledgments

This investigation was partially supported by the international Science and Technology Center in Ukraine.

References

- [1] A. Zuttel, F. Meli and L. Schlapbach, *Z. Phys. Chem.*, **183** (1994) 355.
- [2] F. Meli and L. Schlapbach, *J. Less-Common Met.*, **172–174** (1991) 1252.
- [3] J.J.G. Willems and K.H.J. Buschow, *J. Less-Common Met.*, **129** (1987) 13.
- [4] M.A. Fetchenko, S. Venkatesan and S.R. Ovshinsky, *Pros. Symp. on Hydrogen Storage Materials, Batteries and Electrochemistry*, Arizona, October 14–17, 1991, *Electrochem. Soc. Proc.*, **92-5**, p. 141.
- [5] Yu Xin-Nan and L. Schlapbach, *Int. J. Hydrogen Energy*, **13** (1988) 429.